Ecology and Epidemiology

Temporal and Spatial Development of Bean Rust Epidemics Initiated from an Inoculated Line Source

Donald E. Aylor and Francis J. Ferrandino

Department of Plant Pathology and Ecology, The Connecticut Agricultural Experiment Station, P.O. Box 1106, New Haven, CT 06504.
Accepted for publication 8 August 1988 (submitted for electronic processing).

ABSTRACT

Aylor, D. E., and Ferrandino, F. J. 1989. Temporal and spatial development of bean rust epidemics initiated from an inoculated line source. Phytopathology 79:146-151.

Development of bean rust in time and space was studied during 1986 and 1987 in a 30 × 60-m field containing 77 rows of snap beans. The center row was inoculated and served as a 30-m line source, approximately perpendicular to the prevailing wind. Bean rust pustules were counted on the center leaflet of all trifoliolate leaves of plants at distances of 0.8 to 29.5 m from the source during the course of the epidemics. Primary disease gradients were described well by a power law. As the epidemics progressed, the disease gradients became flatter as a result of secondary spread. The major features of the development of the disease with time (t) and distance from the inoculated source (x), where P is the number of pustules per plant, were described well by plotting $\ln(P)$ vs. $A + r \cdot t - b \cdot \ln(x)$, which collapsed all 19 measured gradients onto a single curve. The parameters A, r, and b are related to the initial level of disease at the start of the epidemic, the rate of increase of the number of pustules with time, and the shape of the gradients in space, respectively.

Additional keywords: disease progress curves, spatial distribution, spore dispersal, *Uromyces appendiculatus*.

Description of the development of plant disease epidemics in time and space is a major goal of plant disease epidemiology. Our present understanding of the spatial dynamics of plant disease epidemics has been advanced by several recent studies (3,8–11,14,15,17). One much-remarked-upon characteristic of disease development is the flattening of disease gradients with time (3,6,8,10,11,14,20). A disease gradient can flatten locally with time for at least two reasons. Firstly, flattening can occur because of a limitation of infection sites, which slows the epidemic near a focus more than at the periphery. Secondly, flattening can result from the exchange of spores between regions with different levels of disease (superposition of spore deposition from sources at several locations), which tends to equalize the rate of disease increase in different parts of the field. In addition, gradients can flatten locally but remain steep along a disease front moving away from the initial

focus. This is evident when the gradient is measured at a constant level of disease (14). However, in order to observe such disease fronts, the experimental field must be large compared to the distance over which spores are dispersed (10,15). A relatively steep spore dispersal gradient is required in order to observe these fronts in the small field plots often used in experiments.

In an important empirical study of crown rust of oats, Berger and Luke (3) showed that graphs of logit(y) vs. log(x), where y is disease severity and x is distance from the source, did not show the flattening of the disease gradient typically seen when log(y) is plotted against log(x). Their findings can be represented by a transformation given by Jeger (8, Table 4, eq. iv), who also showed that this same transformation could linearize data for the incidence of *Septoria nodorum* on wheat (9). The logit transformation accounts for the first mechanism for flattening gradients mentioned above, i.e., it adjusts for the limitation of infection sites (5,19). However, this transformation does not explicitly account for the second mechanism, which should introduce downward curvature into these kinds of graphs. It is possible that the spores from the initial focus of disease overshadowed the superposition of spores from secondary sources throughout the field in determining the disease gradient in the study by Berger and Luke. We will return to this point later in the paper.

The purpose of this paper is to examine the relationship between the increase of the level of disease with time and space during the development of a bean rust epidemic. We will show that disease gradients for bean rust, measured during several generations of the pathogen and over distances of up to 30 m, can be collapsed onto a single curve and explain why, in certain cases, the complications of superposition of spores from distant sources within the field do not strongly affect the overall development of the epidemic.

MATERIALS AND METHODS

Field experiment. Disease gradients were measured in a 30 × 60-m field of snap beans, *Phaseolus vulgaris* cv. Bush Blue Lake 47 (BBL47), at Mt. Carmel, Connecticut, during July–September of 1986 and 1987. Beans were planted in rows (30 m long and 0.8 m wide) approximately perpendicular to the prevailing north-south wind. The experimental field was bordered on the west by four north-south rows of a resistant bean cultivar, which did not support sporulation, and by a 30 × 60-m field planted with alternate rows of BBL47 and the resistant cultivar; the field has been previously described in detail (2). The entire length of the center row (row 0) was inoculated on days 219 and 224 of the year (from 1 January) in 1986 and on days 210 and 215 in 1987; the plants were sprayed with a water suspension of urediniospores of Race 38 (18) of the bean rust pathogen, *Uromyces appendiculatus* (Pers.) Unger (syn. *U. phaseoli* (Pers.) Winter). Weather conditions during the epidemics have been described elsewhere (2).

The amount of disease on a given date was determined by counting the total number of pustules on the center leaflet of all trifoliolate leaves of sampled plants. Three to five plants were selected for counting from the middle 20 m of selected rows. For the final determination in 1987 only, the number of pustules per leaflet was estimated by counting the number of pustules within three to five standard areas (1.5 cm^2) on each leaflet. The area of a sampled leaflet was determined, and counts per leaf were obtained by multiplying the estimated density of pustule counts (per square centimeter) by the area of the leaf (2). For each selected row, we combined the counts from the sampled plants to estimate the average number of pustules per plant (i.e., on the center leaflets of the trifoliolate leaves), which we designated P.

Data analysis. The increase of P in a given row with time was fitted to a logistic law and an exponential law by means of nonlinear regression (12) and was expressed as:

$$P = P_{max}/(1 + \exp[r \cdot (t - t_{1/2})]) \quad (1)$$

$$P = P_0 \exp[r \cdot (t - t_0)] \quad (2)$$

in which P_{max} is the asymptotic value of the logistic model, corresponding to the maximum number of pustules per plant; r is the apparent infection rate; t is time; $t_{1/2}$ is the time when $P = P_{max}/2$; and P_0 is the average number of pustules per plant at time t_0, when the first observations were made.

The increase of P in time and space was examined with an equation of the form given by Jeger (8):

$$\text{logit}(P/P_{max}) = A + r \cdot (t - t_0) - b \cdot \ln(x) \quad (3)$$

in which x is the distance from the focal infection and b is related to the exponent of the power law that is assumed to describe the primary spore dispersal gradients (1,16). In the early stages of an epidemic (i.e., for $P/P_{max} \ll 1$) equation 3 can be represented by

$$\ln(P) = \ln(P_0) + r \cdot (t - t_0) - b \cdot \ln(x) . \quad (4)$$

The parameters in equations 3 and 4 were fitted to the data by nonlinear regression (12). These equations were also fitted to the results of simulation model calculations described below. The "best fit" to the data, as defined by a minimal value for the sum of the squares of the errors (SSE), was approximated by an iterative process.

The form of equation 4 is particularly useful in that the spatial and temporal variations of disease development can be separated. For purposes of later discussion, it is convenient to express equation 4 in the equivalent form

$$P(x, t) = P_0(x)\exp[r \cdot (t - t_0)] \quad (5)$$

$$P_0(x) = P_0(1) \cdot x^{-b} \quad (6)$$

in which $P_0(x)$ is the initial disease as a function of x.

Simulation model. The spread of the disease in space and its progress in time in the experimental field were calculated with a simulation model based on earlier models (10,11,17). The increase in the number of pustules was calculated once for each generation of the pathogen (11). Pustules were assumed to remain infectious throughout the epidemics studied here (27–30 days) (7).

Each pustule was assumed to produce M effective spores at regular intervals of time (the latent period, p). These spores are distributed over plants in the field following rules specified by a spore transport matrix, $T(i - i', j - j')$ (10). The field was represented by a rectangular grid of square boxes, of length ΔL on a side, with I rows and J columns. The indices $i - i'$ and $j - j'$ represent the separation (measured in number of rows and columns) between source and receiver locations. The deposited spores produce secondary pustules, which contribute to the pool of spores during the next generation. If the total number of pustules after n generations in box (i', j') is represented by $N^n_{i'j'}$, then the number of spores that originate from those pustules and are deposited in box (i, j) is

$$S^n_{ij} = M \sum_{i'=1}^{I} \sum_{j'=1}^{J} N^n_{i'j'} T(i - i', j - j') . \quad (7)$$

Because of multiple hits on the same infection sites, only a portion of the spores deposited in box (i, j) will result in pustules (5,19). On the assumption that spores are distributed evenly over N_M possible infection sites within a box, the number of pustules in box (i, j) after n generations is

$$N^{n+1}_{ij} = N_M[1 - (1 - N^n_{ij}/N_M) \cdot \exp(-S^n_{ij}/N_M)] . \quad (8)$$

The spore dispersal transport matrix was assumed to be radially symmetric and based on a power law (1,4,6,16,17). Specifically, $T(i-i', j-j')$, which relates the number of spores deposited in box (i, j) of the computation grid to the number released from box (i', j'), was expressed as (16,17)

$$T = T_0(1 + s/c)^{-B} \quad (9a)$$

where

$$s = \Delta L[(i - i')^2 + (j - j')^2]^{1/2} \quad (9b)$$

in which s is the straight-line distance between the source and the receptor box. The parameter c is of the order of the size of the source region and ensures that T remains finite at $s = 0$ (1,16). We chose $c = 0.5$ m. The parameter B, which determines the steepness of the spore dispersal gradient, was set equal to 2.2, in agreement with an earlier study (4).

The effective multiplication, M, of pustules per generation of the pathogen was adjusted so that after four generations, the model gave numbers of pustules (in row 2) that were similar to those found in the field at the end of the observations. We were guided in our choice of M by the relationship $M = \exp(p \cdot r) - 1$, given by van der Plank (19).

Source geometry. We examined the effect of the finite length of the source (30 m) on the number of pustules with respect to distance from the source, by using our simulation model appropriately modified to simulate an infinitely long line source. The distance s in equation 9b was replaced by $\Delta L \cdot (i - i')$, the value of B was reduced by 1, and only one summation (over i') was required in equation 7. Reducing the value of B by 1 was intended to account approximately for the reduction by 1 in the number of spatial dimensions for spore dispersal, which is required in going from equation 9b, appropriate for a point source, to the form appropriate for an infinite line source (4,6,13). The effect of source geometry on disease gradients was then assessed by comparing the results of the one- and two-dimensional calculations.

We further examined the effect of the finite length of the source on the shape of the primary disease gradient by approximating the spore dispersal transfer function (equation 9) by the following continuous function of distance from the source, which can be integrated in closed form:

$$T' = T_0'[1 + (s^2/C^2)]^{-1} \quad (10)$$

where, now, $s = \sqrt{(x^2 + y^2)}$. The x direction is perpendicular to the line source, and the y direction is parallel to the line source, which lies along the line $x = 0$. The parameter C is also related to the size of the source region but differs numerically from c in equation 9b. We integrated equation 10 in the y direction over the length of the source, W. Along a line at the center of the field ($y = 0$), this integration yields

$$\int_{-W/2}^{W/2} T'\, dy = 2 \cdot T' \cdot C \cdot (1 + x^2/C^2)^{-1/2} \cdot \arctan(W/[2 \cdot C \cdot (1 + x^2/C^2)^{1/2}]) \quad (11)$$

which approximately describes the variation with distance of the primary dispersal gradient. For $x \ll C$, this function is essentially a constant. For $C \leqslant x \ll W$, the function varies approximately as x^{-1}. For $x \gg W$, it varies as x^{-2}.

RESULTS

The rate of increase of disease in both years is described well ($R^2 > 0.95$) by equation 2, where R^2 is the coefficient of determination in the nontransformed space. For almost all of the distances sampled, nonlinear regression by means of either an exponential or a logistic law gives nearly identical fits to P. This indicates that infection sites were not limiting disease development. For example, the regression using the logistic model for observations in row 2 (Fig. 1) sets the asymptote greater than 50,000 pustules, which is about five times larger than the maximum number of pustules observed. It also sets $t^{1/2} > 270$ day, which is beyond the time when observations were made. This agrees with estimated severities, which were less than 15% (on a whole-plant basis) at the end of the epidemics. For the epidemics studied here, either a logit or a log transformation of pustule counts gives essentially identically

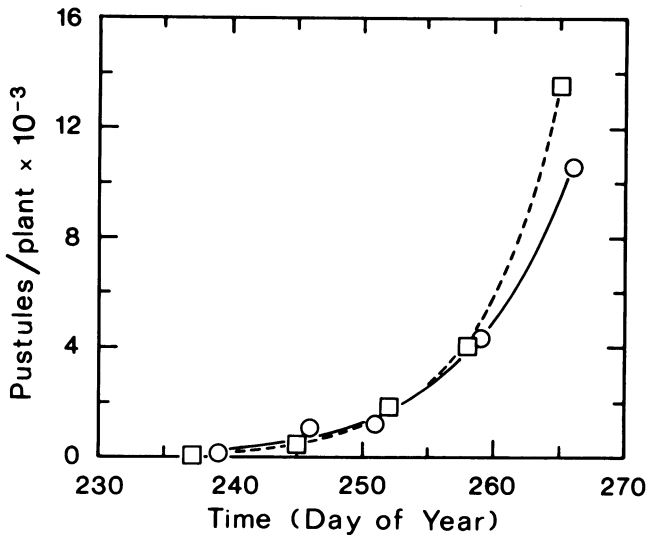

Fig. 1. Increase of the number of pustules per plant with time in the second row south of the inoculated row during 1986 (circles) and 1987 (squares). Pustules were counted only on the center leaflet of the trifoliolate leaves. The lines are nonlinear regression fits of the data to the exponential law $P = P_0 \cdot \exp[r \cdot (t - t_0)]$, where P is the number of pustules per plant, which gave $r = 0.132$ ($R^2 = 0.997$) for 1986 (solid line) and $r = 0.165$ ($R^2 = 0.99$) for 1987 (dashed line).

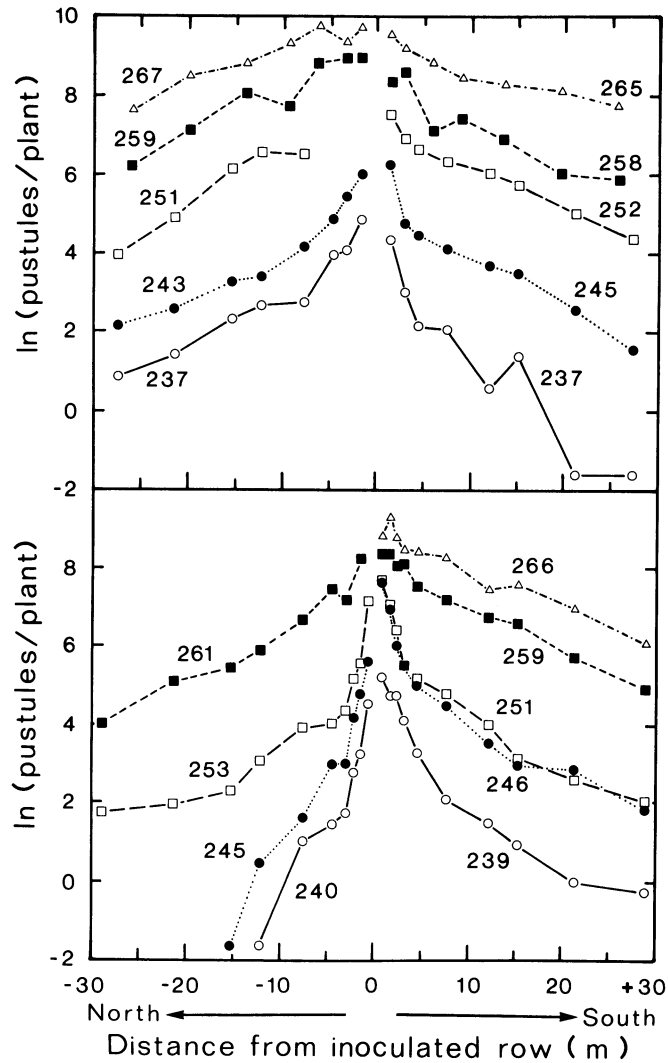

Fig. 2. Variation of ln(P) with x, where x is distance (in meters) from the inoculated row and P is the average number of pustules per plant during the bean rust epidemics in 1986 (bottom panel) and 1987 (top panel). The negative and positive numbers on the abscissa represent distances to the north and south, respectively, of the inoculated row. Each curve is labeled with the day of the year when the counts were made.

shaped curves, and we present our results using a log transformation.

For comparison and for purposes of later discussion, development of the rust epidemics in time and space are plotted versus linear distance, x, from the inoculated row (Fig. 2) and versus $\ln(x)$ (Fig. 3). The gradients tend to be steeper to the north of the source in 1986 and steeper to the south of the source in 1987. In both years, the gradients became flattened as the epidemics progressed. In the plot of $\ln(P)$ vs. x, the initial gradients were concave upward, and later gradients became straighter. In the plot of $\ln(P)$ vs. $\ln(x)$, the initial gradients were approximately straight lines and later gradients became concave downward.

The data collapse onto a single curve (Fig. 4) when the observed values of $\ln(P)$ are plotted versus $\ln(P_0) + r \cdot t - b \cdot \ln(x)$, the theoretical prediction for $\ln(P)$ given by equation 4. The parameters P_0, r, and b were fitted independently for the four sets of data (north and south of the inoculated row for 2 yr) (Table 1). With the exception of the data north of the source in 1986, the values of b, which measure the shape of the disease progress curves, are very similar.

The general shapes of the simulated curves (Fig. 5) are in qualitative agreement with our observations. For all generations after the first, the calculations show a sharp downward bend on the right, which is due to spore loss from the edge of the field. The shape of the curve given by equation 11 (with $W = 30$ m and $C = 0.5$ m) agrees with the two-dimensional calculations for the first generation so closely that the two lines essentially coincide. The transformation given by equation 4 reduces the model calculations into a series of curves, which, taken together, approximate a single curve (Fig. 6), which is qualitatively similar to the curve found by observation (Fig. 4).

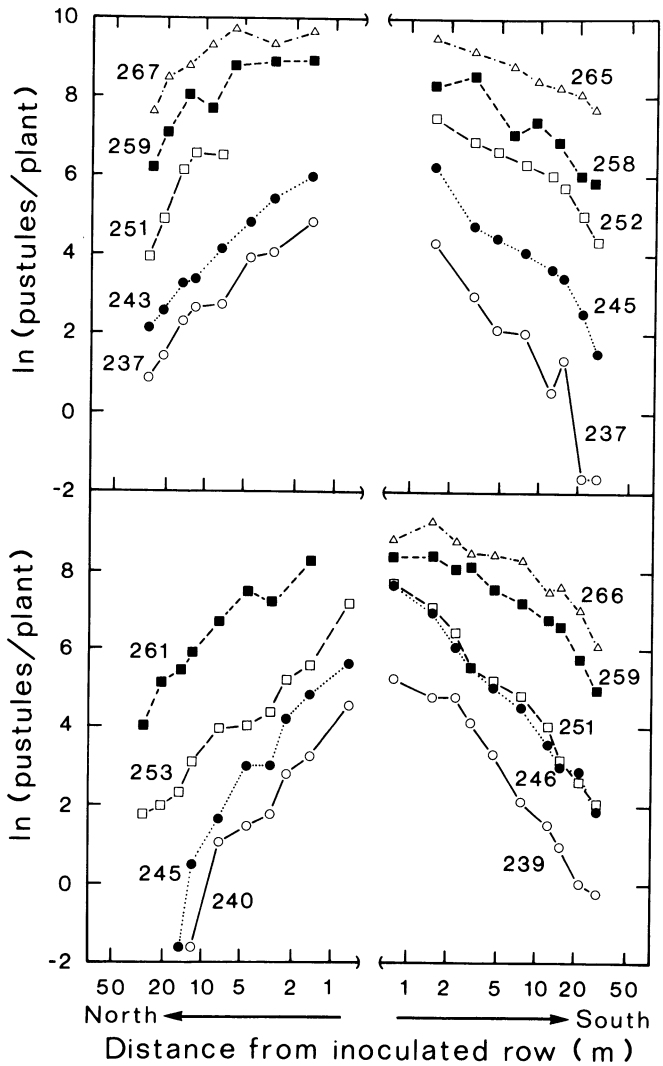

Fig. 3. Variation of $\ln(P)$ with $\ln(x)$, where x is distance (in meters) from the inoculated row and P is the average number of pustules per plant during the bean rust epidemics in 1986 (bottom panel) and 1987 (top panel). The numbers to the left and right of the center of the abscissa represent distances to the north and south, respectively, of the inoculated row. Each curve is labeled with the day of the year when the counts were made.

DISCUSSION

The general course of an epidemic described by equations 3 and 4 can be represented by a series of curves plotted in three dimensions (Fig. 7). These curves represent the progress of a disease for which the exchange of spores between secondary sources of inoculum on distant plants can be ignored. Spores originate from a focus of infection and are deposited on plants at distances according to a power law (equation 6), shown by the curve labeled t_0. Development of the epidemic in time occurs by local multiplication of pustules, which starts from an initial level given by the primary spore dispersal. In this simple model, spore dispersal between plants (i.e., dispersal other than autoinfection) is ignored during the buildup of disease. For a disease that follows these rules, the transformation given by equation 3 should allow observations of disease in space and time to be collapsed onto a single *straight* line on a logit-log plot (9). This situation might also

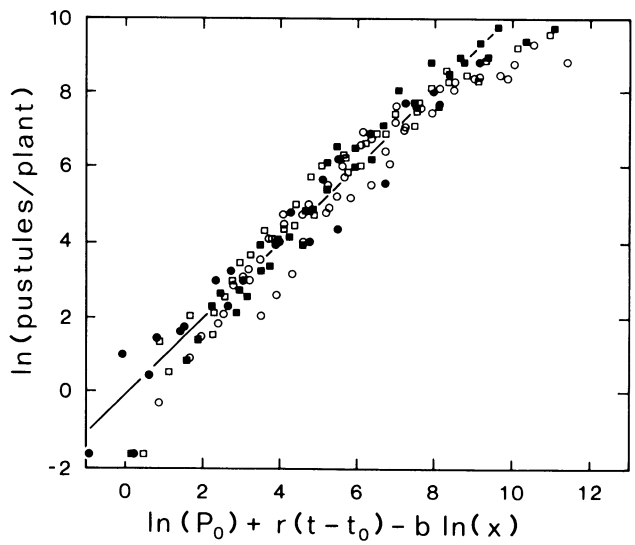

Fig. 4. Relationship between the observed values of $\ln(P)$ and values predicted by equation 4, $\ln(P) = \ln(P_0) + r \cdot (t - t_0) - b \cdot \ln(x)$, with values of the parameters as given in Table 1, for observations in the south half of the field (open circles, 1986; open squares, 1987) and in the north half (solid circles, 1986; solid squares, 1987). The line through the data is the 1:1 line.

TABLE 1. Parameter values obtained by nonlinear regression fitting $\ln(P) = \ln(P_0) + r \cdot (t - t_0) - b \cdot \ln(x)$ to the average counts of rust pustules per plant $[P(x, t)]$ at various distances (x) from an inoculated source and at various times (t) during the course of bean rust epidemics[a]

Year	Direction[b]	P_0[c]	t_0[c] (day)	r (day^{-1})	b	R^2
1986	South	166.7	239	0.19	1.26	0.929
	North	32.9	240	0.31	1.75	0.949
1987	South	60.5	237	0.26	1.18	0.944
	North	165.0	237	0.21	1.05	0.956

[a] Pustules were counted only on the center leaflet of the trifoliolate leaves. The equation was fitted separately for counts made north and south of the inoculated row for 2 yr.

[b] Direction in which gradients were measured from the inoculated row, which was in the center of the field. The prevailing winds were from the north and south (2).

[c] The parameter P_0 is the value of P at $t = t_0$ and $x = 1$ m, where t_0 is day of the year of the first observations.

apply approximately when the initial source of inoculum persists and increases without limit throughout the course of the epidemic. In this case, spore dispersal from the initial infection site might dominate disease development during the entire epidemic.

The bean rust epidemics studied here and the oat crown rust epidemics studied by Berger and Luke (3) encompassed several generations of the pathogen and allowed ample opportunity for spore dispersal between all infected plants in the field. In these cases, the epidemics should be governed by equations 7–9, where the local increase of disease with time also depends upon the superimposed effect of the deposition of spores originating from distant sources. This effect tends to flatten gradients (11) and gives a downward curvature on either a logit-log or a log-log plot. The magnitude of this effect tends to become less evident as distance from the focus increases. The effect of an exchange of spores between distant plants was evident both in our data (downward curvature, Fig. 3) and in the results calculated by our model (Fig. 5). The data of Berger and Luke appear to show less curvature than the present study. Part of this difference may be due to the relatively small distances examined by Berger and Luke (1.2–4.9 m), compared to the range in the present study (0.75–30 m). It is also possible that spore transport between plots (3) may have suppressed curvature that should have been caused by superposition of spore sources within a given plot.

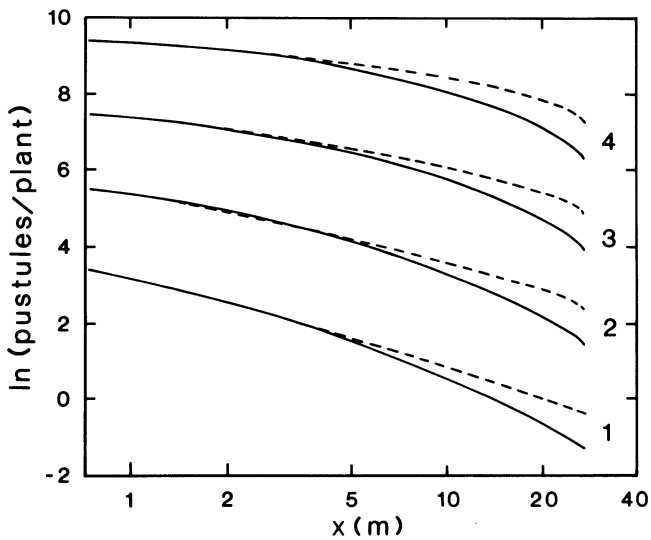

Fig. 5. Progress of bean rust simulated by the numerical model for the south half of the field in 1986. The sets of curves labeled 1–4 represent the results for the four generations of the pathogen following the initial spore dispersal from the inoculated source row for the one-dimensional simulation (dashed lines) and the two-dimensional simulation (solid lines). The model results were forced to agree for row 1 at 0.76 m.

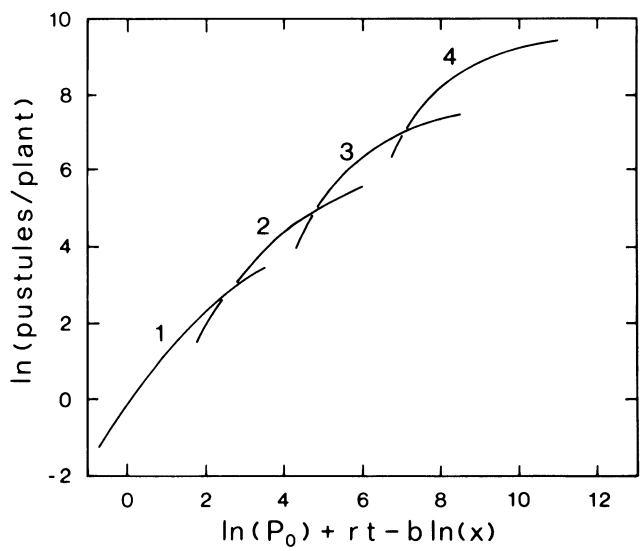

Fig. 6. Values of $\ln(P)$ obtained from the two-dimensional simulation model for disease development in the south half of the field in 1986 plotted versus $\ln(P_0) + r \cdot t - b \cdot \ln(x)$ (from equation 4), where $t = n \cdot p$ and the parameters were fitted by nonlinear regression. The numbers next to the curves represent generations 1–4 of the pathogen.

Even though the curves obtained from our model for each generation of the pathogen exhibit considerable curvature, when all generations are taken together, the overall course of the simulated epidemic approximates a straight line. This helps to illustrate how, in spite of the complication of the superposition of spores from distant sources, most of the variation in our data can be explained by equation 4, which, strictly speaking, should only hold for a disease where spores are dispersed to other plants only once and where disease multiplication results from autoinfection.

Our bean rust epidemics originated from inoculated sources, which remained infectious throughout the course of the epidemic. It is likely that the contribution of spores from this source dominated disease development during much of the epidemic. Likewise, it is possible that spores released from inoculated sources dominated the development of oat crown rust observed by Berger and Luke (3). A strongly inoculated focus establishes the primary gradient, and, as long as it persists, all spores released by the original source throughout the course of the epidemic tend to reinforce the primary gradient. Furthermore, with the relatively steep spore dispersal gradients associated with rust diseases (1,4) autoinfection of the host plant is a major contributor to the development of disease in time. Assuming uniform conditions for disease development throughout the field, this autoinfection does not change the shape of the gradient but simply increases the level of disease in a parallel manner throughout the field. This also reinforces the shape of the primary gradient. Although the exchange of spores between plants in other regions of the field contributes to changing the disease gradient, this effect may be overshadowed by the other two effects. Fig. 7 is qualitatively

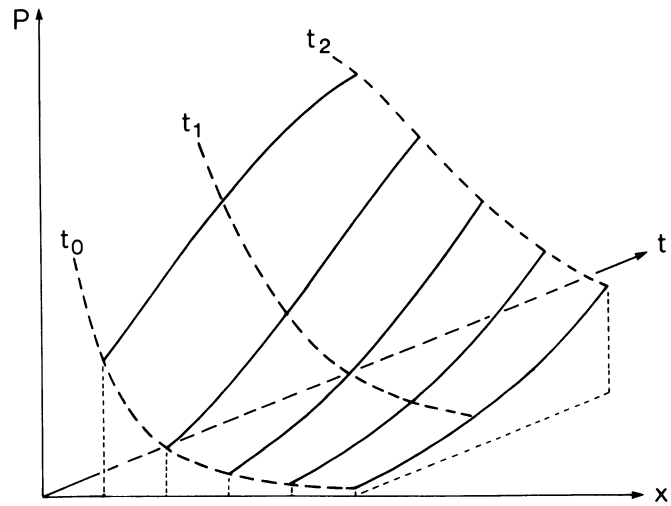

Fig. 7. Schematic of the development of disease in space and time represented by equation 3. The solid lines represent time courses of disease at constant distances from the source (at $x = 0$); the dashed lines represent spatial variation of disease at constant times, starting from the initial appearance of pustules, which were induced by spores dispersed from the inoculated source one latent period earlier. The dashed curve labeled t_0 is described by a power law (equation 6). In this diagram, initial inoculum levels at small distances from the focus were high, and the logistic model is required in order to describe disease progress at these distances. At the farthest distances, however, inoculum levels were low, and disease progress can be described well by approximating the logit by $\ln(P)$, as in equation 4. The dashed curves labeled t_1 and t_2 show flattening of the central region (small x) caused by the limited number of infection sites, which is accounted for by the logit transformation. Superposition of spores from spatially distributed sources has a similar effect of flattening the gradients but is not explicitly accounted for by either equation 3 or equation 4.

correct in describing situations with both a strong focal source of inoculum and very steep spore dispersal gradients near the source, and it is therefore not surprising that equation 3 (3) and equation 4 (in the present study) explain most of the behavior of these epidemics. For an epidemic initiated by a source having a relatively short infectious period (much less than the duration of the epidemic), however, the effect of the initial source may not dominate the epidemic as strongly as it apparently did in the present case, and these equations may not describe the situation nearly as well.

The bean plants continued to increase in leaf area up to the end of our observations, disease severity remained relatively low (below 15%), and infection sites apparently were not limiting for disease development. Thus, we were able to apply equation 4. For other crops, or other epidemics, infection sites may become limiting, and then equation 3 should be applied. This is clearly the case for oat crown rust, studied by Berger and Luke (3), and for potato late blight, studied by Minogue and Fry (15).

The considerable amount of the curvature in the plots of our data (Fig. 3) is apparently due to the finite length of the line source. This can be seen by comparing the results from our one- and two-dimensional simulation models (Fig. 5). Although the effects of superposition of spores originating from distant sources is evident in the one-dimensional results (dashed lines), the downward curvature is not very strong. The two-dimensional computation (solid lines) shows much greater downward curvature. This is mainly due to the "changing" dimensionality of the dispersal as distance from the line source increases (equation 11). Close to the center of a line source, the transport function is approximately one-dimensional, with a slope of -1. On the other hand, at great distances from a finite-length line source, the transport function becomes approximately two-dimensional, with a slope of -2. This behavior is evident in our simulated results. The shape of the two-dimensional simulation results for the first generation is matched almost exactly by equation 11. Thus, most of the nonlinearity observed in the transformed data is due to the finite length (30 m) of the source. The sharp downward hook on the ends of the curves away from the inoculated source is an edge effect caused by loss of spores, without return, from plants near the field edge.

In conclusion, the major features of the development of bean rust epidemics originating from a focus of infection seem to be described well by a relationship of the form $\ln(P) = \ln(P_0) + r \cdot t - b \cdot \ln(x)$. For the epidemics studied here, the parameters P_0, r, and b are related in a physically realistic way to the initial level of disease at the start of the epidemic, the rate of increase of the number of pustules with time, and the shape of the gradients in space, respectively. It seems possible that this kind of mathematical transformation might be applicable for the spread of disease from a focus of infection for other aerially transmitted diseases in which the pathogen has a long infectious period, which allows the initial focus to dominate the course of the epidemic, and in which the crop continues to grow so that uninfected host tissue does not become limiting.

LITERATURE CITED

1. Aylor, D. E. 1987. Deposition gradients of urediniospores of *Puccinia recondita* near a source. Phytopathology 77:1442-1448.
2. Aylor, D. E. 1988. Development of bean rust epidemics in a field planted with alternate rows of a resistant and a susceptible snap bean cultivar. Phytopathology 78:1210-1215.
3. Berger, R. D., and Luke, H. H. 1979. Spatial and temporal spread of oat crown rust. Phytopathology 69:1199-1201.
4. Ferrandino, F. J., and Aylor, D. E. 1987. Relative abundance and deposition gradients of clusters of urediniospores of *Uromyces phaseoli*. Phytopathology 77:107-111.
5. Gregory, P. H. 1948. The multiple-infection transformation. Ann. Appl. Biol. 35:412-417.
6. Gregory, P. H. 1968. Interpreting plant disease dispersal gradients. Annu. Rev. Phytopathol. 6:189-212.
7. Imhoff, M. W., Leonard, K. J., and Main, C. E. 1982. Patterns of bean rust lesion size increase and spore production. Phytopathology 72:441-446.
8. Jeger, M. J. 1983. Analysing epidemics in time and space. Plant Pathol. 32:5-11.
9. Jeger, M. J., Jones, D. G., and Griffiths, E. 1983. Disease spread of non-specialised fungal pathogens from inoculated point sources in intraspecific mixed stands of cereal cultivars. Ann. Appl. Biol. 102: 237-244.
10. Kampmeijer, P., and Zadoks, J. C. 1977. EPIMUL, a Simulator of Foci and Epidemics in Mixtures of Resistant and Susceptible Plants, Mosaics and Multilines. Centre for Agricultural Publishing and Documentation, Wageningen, Netherlands. 50 pp.
11. Kiyosawa, S., and Shiyomi, M. 1972. A theoretical evaluation of the effect of mixing resistant variety with susceptible variety for controlling plant diseases. Ann. Phytopathol. Soc. Jpn. 38:41-51.
12. Marquardt, D. W. 1963. An algorithm for least-squares estimation of nonlinear parameters. J. Soc. Ind. Appl. Math. 11:431-441.
13. McCartney, H. A., and Bainbridge, A. 1984. Deposition gradients near to a point source in a barley crop. Phytopathol. Z. 109:219-236.
14. Minogue, K. P. 1986. Disease gradients and the spread of disease. Pages 285-310 in: Plant Disease Epidemiology. K. J. Leonard and W. E. Fry, eds. Macmillan, New York.
15. Minogue, K. P., and Fry, W. E. 1983. Models for the spread of plant disease: Some experimental results. Phytopathology 73:1173-1176.
16. Mundt, C. C., and Leonard, K. J. 1985. A modification of Gregory's model for describing plant disease gradients. Phytopathology 75:930-935.
17. Mundt, C. C., Leonard, K. J., Thal, W. M., and Fulton, J. H. 1986. Computerized simulation of crown rust epidemics in mixtures of immune and susceptible oat plants with different genotype unit areas and spatial distributions of initial disease. Phytopathology 76:590-598.
18. Stavely, J. R. 1984. Pathogenic specialization in *Uromyces phaseoli* in the United States and rust resistance in beans. Plant Dis. 68:95-99.
19. Van der Plank, J. E. 1963. Plant Diseases: Epidemics and Control. Academic Press, New York. 349 pp.
20. Waggoner, P. E. 1952. Distribution of potato late blight around inoculum sources. Phytopathology 42:323-328.